Chemical Science

ROYAL SOCIETY OF CHEMISTRY

EDGE ARTICLE

Cite this: *Chem. Sci.*, 2022, **13**, 2303

All publication charges for this article have been paid for by the Royal Society of Chemistry

Received 1st January 2022
Accepted 26th January 2022

DOI: 10.1039/d2sc00002d

rsc.li/chemical-science

Unraveling the reactivity of a cationic iminoborane: avenues to unusual boron cations†

Rui Guo,[a] Xin Zhang,[b] Tong Li,[a] Qianli Li,[c] David A. Ruiz,[b] Liu Leo Liu,[b] Chen-Ho Tung[a] and Lingbing Kong*[ad]

A cationic terminal iminoborane [Mes*N≡B ← IPr_2Me_2][$AlBr_4$] ($3^+[AlBr_4]^-$) (Mes* = 2,4,6-tri-*tert*-butylphenyl and IPr_2Me_2 = 1,3-diisopropyl-4,5-dimethylimidazol-2-ylidene) has been synthesized and characterized. The employment of an aryl group and N-heterocyclic carbene (NHC) ligand enables $3^+[AlBr_4]^-$ to exhibit both B-centered Lewis acidity and BN multiple bond reactivities, thus allowing for the construction of tri-coordinate boron cations 5^+–12^+. More importantly, initial reactions involving coordination, addition, and [2 + 3] cycloadditions have been observed for the cationic iminoborane, demonstrating the potential to build numerous organoboron species *via* several synthetic routes.

Introduction

Exploration of boron cations has attracted extensive attention not only due to their unique bonding environments and electronic configurations but also due to their potential applications in bond activation and catalysis.[1,2] Generally, boron cations can be classified into borinium $[R_2B]^+$, borenium $[R_2BL]^+$, and boronium $[R_2BL_2]^+$ cations based on the coordination number of boron (Fig. 1a). By installing π-donating ligands at the boron atom to compensate for the inherent electron deficiency, a few borinium ions have been isolated since the first report of diamido-substituted boron cations **I** and **II** by the Nöth group (Fig. 1b).[3] Subsequently, Stephan and coworkers obtained the persistent borinium ion **III** supported by phosphoraniminato groups.[4] In 2014, a seminal report on the synthesis of dimesityl boron cation **IV** was published by Shoji *et al.*[5] **IV** exhibits high Lewis acidity and electrophilic reactivity towards CO_2, CS_2, H_2 and Et_3SiH.[6] In addition, twofold 1,2-carboration of diphenylacetylene with **IV** afforded divinylborinium ion **V**, in which the positive charge is delocalized over the entire π-conjugated system.[7] More recently, the Inoue group demonstrated the asymmetric borinium ion **VI** ligated by imidazolin-2-imino and silyl substituents.[8]

Cationic boron species of type $[R_nE{\equiv}B]^+$ possess different bonding characters from classical boron cations and should be versatile reagents for organic synthesis through the functionalization of multiple bonds.[9,10] Nevertheless, such species are still hitherto unknown. Even with Lewis base stabilization, only two corresponding $[R_nE{\equiv}BL]^+$ and $[R_nE{\equiv}BL_2]^+$ derivatives,

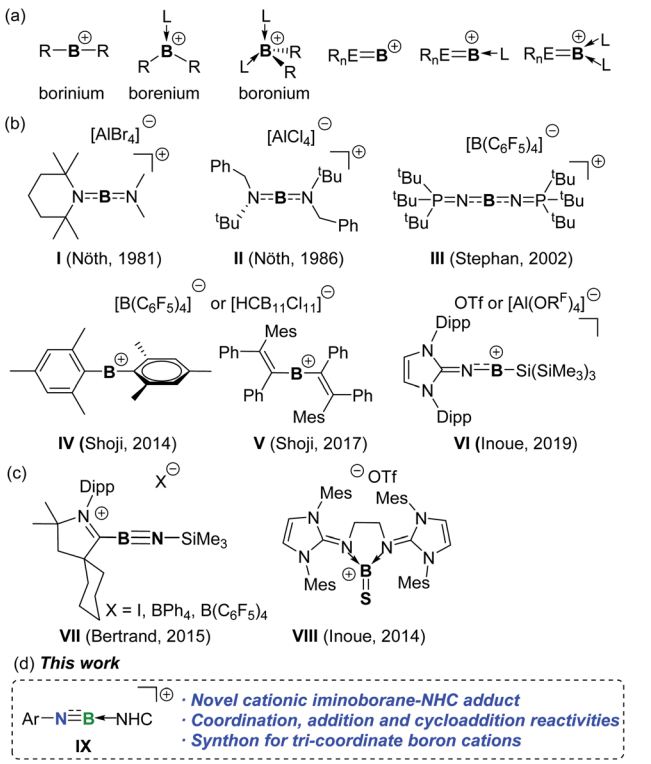

Fig. 1 (a) Boron cations. (b) Structurally characterized borinium ions. (c) Cationic unsaturated boron compounds. (d) This work.

[a]*School of Chemistry and Chemical Engineering, Shandong University, Jinan 250100, P. R. China. E-mail: konglb@sdu.edu.cn*

[b]*Department of Chemistry and Shenzhen Grubbs Institute, Southern University of Science and Technology, Shenzhen 518055, P. R. China*

[c]*School of Chemistry and Chemical Engineering, Liaocheng University, Liaocheng 252059, P. R. China*

[d]*State Key Laboratory of Elemento-Organic Chemistry, Nankai University, Tianjin 300071, P. R. China*

† Electronic supplementary information (ESI) available. CCDC 2078017–2078022; 2109192–2109195. For ESI and crystallographic data in CIF or other electronic format see DOI: 10.1039/d2sc00002d

exemplified by iminoboryl-CAAC adducts **VII** and cationic thioxoborane **VIII**, have been described by the Bertrand, Stephan and Inoue groups, respectively (Fig. 1c).[11,12] **VII-I** with an iodide counter anion is in equilibrium with the neutral idodoiminoborane in solution, which alternatively served as a dipole to cyclize with CO_2. Comparatively, **VII-BPh$_4$** and **VII-B(C$_6$F$_5$)$_4$** retaining the cationic structure both in the solid-state and in solutions do not exhibit dipole reactivity and are inert toward CO_2. Neutral iminoboranes are extensively employed as synthons for constructing organoboron compounds through addition and cycloaddition reactions.[13] Therefore, development of persistent yet highly reactive cationic counterparts and unravelling their reactivity would provide new avenues to cationic boron species. Herein, we report the access to the cationic iminoborane **IX** supported by an NHC, as well as its utility for constructing unusual B-containing frameworks (Fig. 1d).

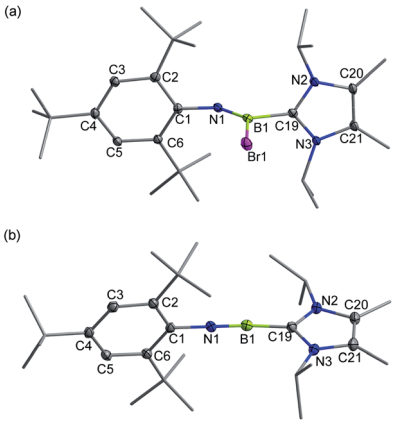

Fig. 2 Solid-state structures of **2** (a) and **3**$^+$[AlBr$_4$]$^-$ (b). The counterion and hydrogen atoms are omitted for clarity. Thermal ellipsoids are set at the 30% probability level.

Results and discussion

Synthesis and characterization of 3$^+$[AlBr$_4$]

Recently, we demonstrated a facile approach for the synthesis of iminoborane-NHC complexes by employing NHCs as Brønsted bases and ancillary ligands.[14] In an analogous fashion, addition of two equiv. of 1,3-diisopropyl-4,5-dimethylimidazol-2-ylidene (IPr_2Me_2) into Mes*NHBBr$_2$ **1** in toluene afforded compound **2** as colorless crystals in 56% yield (Scheme 1). The multi-nuclear NMR spectroscopic studies coupled with single crystal X-ray diffraction confirmed the formulation of **2** to be Mes*N=B(Br)IPr_2Me_2 (^{11}B NMR: 9.4 ppm). In the solid state, the boron center of **2** adopts a planar geometry with the sum of angles at 359.9°. The Mes* and IPr_2Me_2 groups are located on the opposite sides of the B1=N1 double bond (Fig. 2a).

Halide abstraction of **2** was next examined. We reacted **2** with an equal molar amount of $AlBr_3$ in toluene at ambient temperature for 5 minutes to obtain colorless solids of **3**$^+$[AlBr$_4$]$^-$ quantitatively. The ^{11}B NMR spectrum of **3**$^+$ shows a broad signal at 6.9 ppm, which is close to the chemical shifts seen for the iminoboranes ArB≡NR (2.8–4.3 ppm),[13,15] borinium **III** (11.1 ppm)[4] and cationic iminoboranes **VII**[11] (7.7 and 7.4 ppm), but strongly upfield-shifted with respect to those of two-coordinate boron cations **I**, **II**, **IV** and **V** (36.7, 38.7, 93.3 and 74.0 ppm, respectively).[3,5,7] A sharp singlet peak at 80.8 ppm assigned to [AlBr$_4$]$^-$ was observed in the ^{27}Al NMR spectrum, demonstrating the smooth bromide abstraction of **2** by $AlBr_3$. Species **3**$^+$[AlBr$_4$]$^-$ exhibits high thermal stability under an inert atmosphere and does not decompose even upon heating at 80 °C for 24 h in C_6D_6 (Fig. S71†).

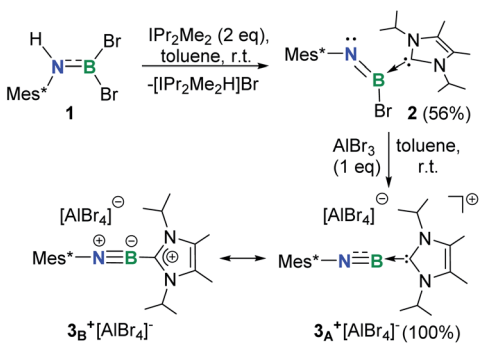

Scheme 1 Synthesis of **2** and **3**$^+$[AlBr$_4$]$^-$ (Mes* = 2,4,6-tri-*tert*-butylphenyl).

Single crystal X-ray diffraction unambiguously confirmed the ionic nature of **3**$^+$[AlBr$_4$]$^-$ (Fig. 2b). The B1 atom is ligated with IPr_2Me_2 and well-separated from the counterion [AlBr$_4$]$^-$ with a distance of 4.2575(3) Å between the B1 and the closest bromine atom of the [AlBr$_4$]$^-$ anion, which is much longer than the sum of the van der Waals radii (2.04 Å).[16] The structure of **3**$^+$ shows an essentially linear C1–N1–B1–C19 core with slight bending at the N1 (178.6(4)°) and B1 (173.6(4)°) atoms, indicative of sp-hybridization of these two atoms. The B1–N1 bond length of 1.224(5) Å in **3**$^+$ was found to be identical to those of **VII**[11] (1.229(3), 1.218(4) and 1.192(5) Å) within experimental uncertainty. In addition, the contracted B1–C19 (1.527(5) Å) and similar C1–N1 (1.389(4) Å) bond lengths in comparison to those in **2** (1.605(6) Å and 1.379(5) Å, respectively) were observed.

To further understand the electronic structure of **3**$^+$, DFT calculations at the B3LYP/6-311G* level of theory were performed. The calculated geometrical parameters agree well with those observed for the crystal structure of **3**$^+$. The ^{11}B NMR chemical shift (5.8 ppm) obtained from GIAO calculations is consistent with the experimental value (6.9 ppm, Fig. S82†). The Wiberg Bond Index (WBI) for the B–N bond in **3**$^+$ is 1.98 (Table S2†), which is smaller than that of **VII** (2.10, Table S3†), while those for the C1–N1 and B1–C19 bonds are 1.05 and 0.94, respectively. The natural population analysis (NPA) shows that the boron atom has a positive charge of +0.75, whereas the N1 atom is negatively charged (−0.70 a.u.) (Fig. 3a and Table S4†), suggesting the pronounced polar nature of the B–N triple bond. Indeed, natural bond orbital (NBO) analysis reveals one σ- and two π-bonding features of the BN unit with significant contribution from the N atom (76%, 76% and 74%, respectively, Table S5†). The Mes* and IPr_2Me_2 groups bear +0.28 and +0.67 charges, respectively. Furthermore, second-order perturbation

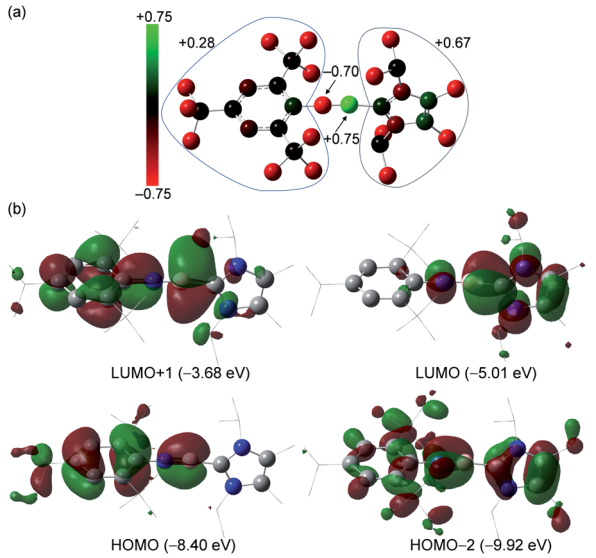

Fig. 3 (a) Natural population analysis for 3^+. (b) Selected molecular orbitals for 3^+. Isovalue = 0.03.

analysis confirmed the electronic conjugation between the B≡N triple bond and Mes* as well as imidazole rings with stabilization energies of 13.9 and 6.9 kcal mol^{-1}, respectively (Fig. S85†).

The HOMO and HOMO−2 of 3^+ represent out-of-plane and in-plane B–N π-bonding orbitals, with contributions from π orbitals of Mes* or imidazole moieties, whereas the LUMO and LUMO+1 predominately involve their π*-components (Fig. 3b). The UV/Vis and IR spectroscopic analyses of $3^+[AlBr_4]^-$ were also carried out. The former showed no detectable absorption between 240 and 400 nm (Fig. S15†), whereas the signal at a shorter wavelength (<240 nm) was too noisy or saturated for a reliable assignment. The latter measured in the solid state exhibited a characteristic peak at $\tilde{\nu}$ = 2004 cm^{-1} for the B≡N stretching vibration (Fig. S16†), which is comparable to that for ^{t}BuB≡N^{t}Bu (2018 cm^{-1})[17] and is in good agreement with the calculated result (2008 cm^{-1}, Fig. S84†).

Examination of the Lewis-acidity of $3^+[AlBr_4]^-$

The Lewis-acidity of $3^+[AlBr_4]^-$ was first evaluated by computing its global electrophilicity index (GEI). The GEI value at the B3LYP/def2-TZVP level of theory was calculated to be 2.467 (Fig. S89†), which is slightly smaller than that for BCl_3 (2.766).[18] Next, the reactivity of $3^+[AlBr_4]^-$ towards different Lewis bases was probed. It was demonstrated that hard halide ions such as chloride and bromide readily add to the boron center of $3^+[AlBr_4]^-$. Specifically, treatment of $3^+[AlBr_4]^-$ with one equiv. of [PPN]Cl (PPN = Ph_3P=N=PPh_3) or $[Ph_4P]Br$ in toluene at ambient temperature gave the respective B-halogen substituted iminoboranes **4** and **2** smoothly (Scheme 2). The boron atom in **4** was observed at 12.8 ppm in the ^{11}B NMR spectrum and the single-crystal X-ray analysis elucidated that **4** adopts a formal *Z* configuration similar to compound **2** (Fig. 4a). The B1–N1 bond length (1.305(7) Å) in **4** compares well with that for **2** (1.296(6) Å). Both values are longer than the B≡N triple bond length in 3^+ (1.224(5) Å), illustrating the decreased B–N bond strength in iminoborane-NHC complexes **2** and **4**.

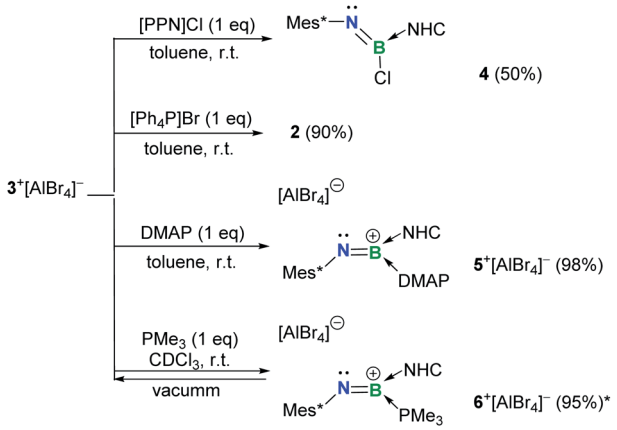

Scheme 2 Reactivity of $3^+[AlBr_4]^-$ toward bases (*NMR yield; NHC = IPr_2Me_2 = 1,3-diisopropyl-4,5-dimethylimidazol-2-ylidene; PPN = Ph_3P=N=PPh_3).

As for the neutral Lewis bases, 4-dimethylaminopyridine (DMAP) and trimethylphosphine (PMe_3) were employed (Scheme 2). Addition of DMAP quantitatively afforded the corresponding cationic terminal iminoborane $5^+[AlBr_4]^-$ (^{11}B NMR: 15.4 ppm) in the coordination sphere of two different Lewis bases. The solid-state structure of 5^+ revealed that the DMAP coordination causes the B1 and N1 atoms to be sp^2-hybridized and results in a twisted C1–N1–B1–C19 skeleton (∠C1–N1–B1 = 139.9(3)°; ∠N1–B1–C19 = 123.2(3)°; Fig. 4b). Accordingly, the B1–N1 bond length of 1.323(4) Å is markedly longer than that of 3^+ (1.224(5) Å) and its WBI is calculated to be 1.55 (Table S6†). In sharp contrast, the coordination of PMe_3

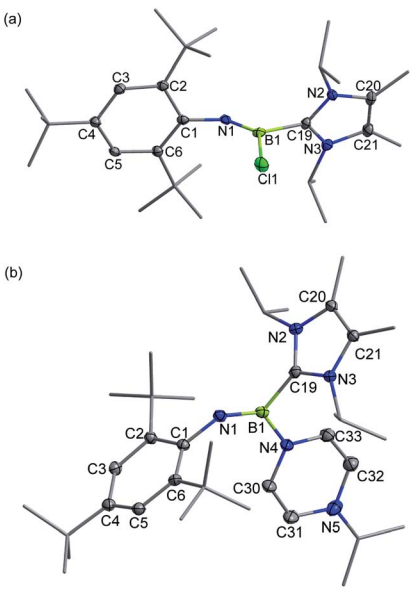

Fig. 4 Solid-state structures of **4** (a) and 5^+ (b). The counterion and hydrogen atoms are omitted for clarity. Thermal ellipsoids are set at the 30% probability level.

with $3^+[AlBr_4]^-$ was found to be reversible. Although multinuclear NMR spectroscopic investigations clearly showed the formation of an adduct $6^+[AlBr_4]^-$, evaporation of the $CDCl_3$ solution of $6^+[AlBr_4]^-$ regenerated species $3^+[AlBr_4]^-$. Indeed, PMe_3 is much more fragile than NHC in 6^+ judging from the corresponding bond dissociation energies (BDEs) of 3.9 and 41.8 kcal mol^{-1}, respectively (Fig. S90†).

1,2-Addition of $3^+[AlBr_4]^-$

The addition of unactivated C–H bonds across iminoboranes to form aminoboranes is extremely challenging. It was found that in the presence of sodium cyanate (NaOCN), $3^+[AlBr_4]^-$ converted into the product $7^+[AlBr_4]^-$ (^{11}B NMR: 40.8 ppm) at 50 °C (Scheme 3). Both NMR spectroscopic and X-ray single-crystal diffraction studies confirmed $7^+[AlBr_4]^-$ to be a cyclic aminoborenium formed *via* an intramolecular C–H bond addition across the B≡N triple bond (Fig. 5a). NaOCN likely acts as a Lewis-base for coordination activation of the B≡N bond to enhance the basicity of N for capturing a proton from the methyl group. Note that a neutral three-coordinate borane enabled intramolecular C–H activation affording borocycles has been described by the Knochel research group.[19] In addition, intermolecular addition proceeded smoothly between $3^+[AlBr_4]^-$ and more acidic acetonitrile at ambient temperature to give the acyclic aminoborenium $8^+[AlBr_4]^-$ (^{11}B NMR: 37.2 ppm; Fig. 5b). It is proposed that this transformation may occur in successive steps involving acetonitrile complexation, proton migration and rearrangement of an aza-allene intermediate (Fig. S81†).[20] Both reactions formed anti-addition products.

Inspired by a few successful examples of catalyst-free transfer hydrogenation (TH) of unsaturated compounds,[21] the reactions of $3^+[AlBr_4]^-$ with $H_3N{\cdot}BH_3$ or $Me_2HN{\cdot}BH_3$ were also conducted. The conversions were complete within half an hour at ambient temperature, generating the corresponding aminoborenium salt $9^+[AlBr_4]^-$ (^{11}B NMR: 34.1 ppm) with concomitant formation of the respective borazine and cyclodiborazane as the by-products (Fig. S72 and S73†). The solid-state structure of $9^+[AlBr_4]^-$ revealed its *trans* stereochemistry (Fig. 5c), which is consistent with Braunschweig's results on TH of neutral

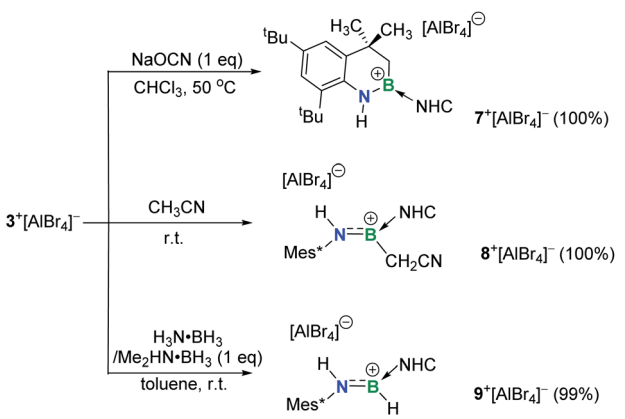

Scheme 3 1,2-Addition of $3^+[AlBr_4]^-$ (NHC = IPr_2Me_2 = 1,3-diisopropyl-4,5-dimethylimidazol-2-ylidene).

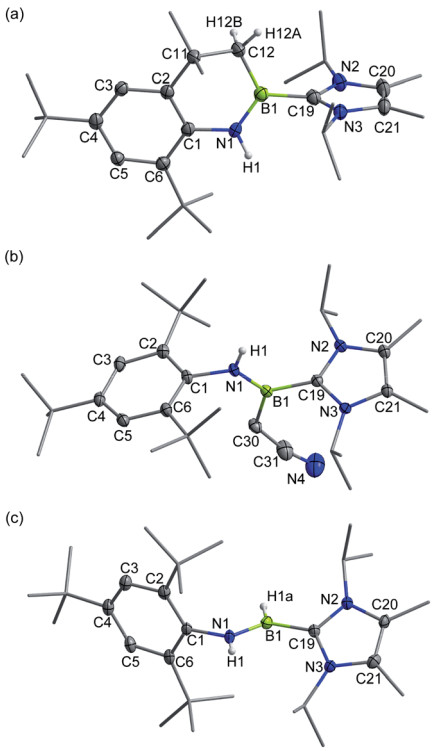

Fig. 5 Solid-state structures of 7^+ (a), 8^+ (b) and 9^+ (c). The counterion and hydrogen atoms except C12–H12A, C12–H12B, N1–H1 and B1–H1a are omitted for clarity. Thermal ellipsoids are set at the 30% probability level.

iminoboranes with $H_3N{\cdot}BH_3$.[22] Deuterium labelling experiments using $H_3N{\cdot}BD_3$, $D_3N{\cdot}BH_3$ and $D_3N{\cdot}BD_3$ resulted in deuterium incorporation at boron, nitrogen and both boron and nitrogen atoms, respectively, as evidenced by ^{2}H NMR with characteristic peaks at 6.64 ppm (N–D) and 4.78 ppm (B–D) (Fig. S74†). This confirmed the polarity match mechanism of TH to $3^+[AlBr_4]^-$. This is different from the aminoborane $iPr_2N{=}BH_2$, which readily undergoes reverse TH with $Me_2HN{\cdot}BH_3$,[23] and no further hydrogenation of species $9^+[AlBr_4]^-$ to amineboronium could be observed in the presence of excess $H_3N{\cdot}BH_3$ or $Me_2HN{\cdot}BH_3$ under heating conditions (Fig. S75†).

[2 + 3] cycloaddition of $3^+[AlBr_4]^-$

The polar B≡N bond also enables the cycloaddition of $3^+[AlBr_4]^-$. Nitrone-, azide- and diazomethane-type 1,3-dipolar systems were thus employed.[24] Treatment of $3^+[AlBr_4]^-$ with one equiv. of *N-tert*-butyl-alpha-phenylnitrone smoothly resulted in the formation of colorless crystals of $10^+[AlBr_4]^-$ (^{11}B NMR: 25.2 ppm; Scheme 4), which were elucidated to be a cationic oxadiazaborolidine species with the newly formed C–N and B–O bonds (Fig. 6a).

When $3^+[AlBr_4]^-$ was treated with trimethylsilyl azide (Me_3SiN_3) in toluene, a white precipitate of **11** was formed immediately. The ^{11}B NMR of **11** showed a signal at 26.0 ppm, whereas ^{1}H NMR revealed that no Me_3Si– group was in the product. Single crystal X-ray diffraction revealed **11** to be a zwitterionic tetraazaborole species with cationic boron and

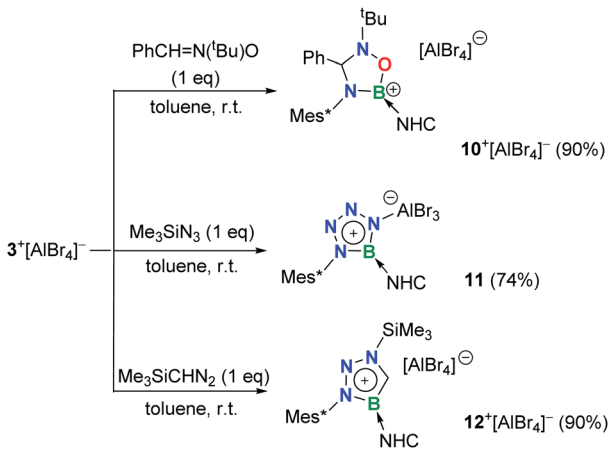

Scheme 4 [2 + 3] cycloaddition of $3^+[AlBr_4]^-$ (NHC = IPr_2Me_2 = 1,3-diisopropyl-4,5-dimethylimidazol-2-ylidene).

anionic aluminium centers (Fig. 6b), resulting from a [2 + 3] cycloaddition and subsequent Al/Si exchange as well as Me_3SiBr elimination. With respect to those of 1,4-diphenyl-5-terphenyltetraazaborole reported by the Braunschweig group,[25] **11** features comparable B–N bond lengths (avg. 1.432 Å) and N–N double bond length (1.276(6) Å) as well as an essentially planar BN_4 five-membered ring (the mean deviation from the plane is 0.0186 Å).

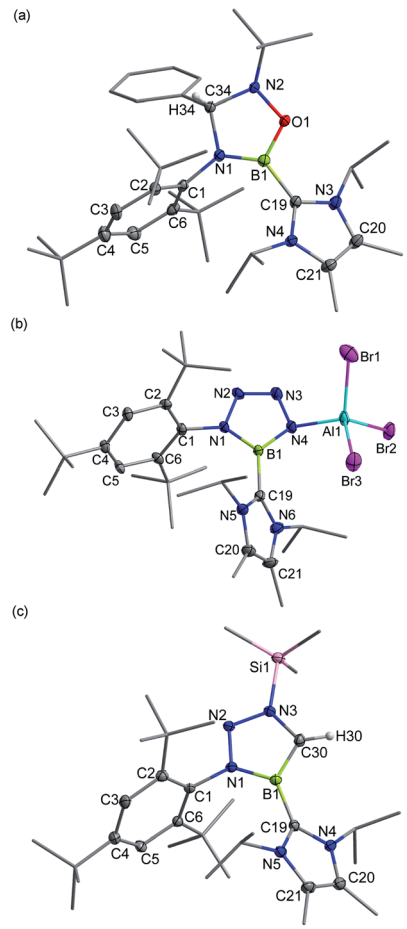

Fig. 6 Solid-state structures of 10^+ (a), **11** (b) and 12^+ (c). The counterion and hydrogen atoms except C34–H34 and C30–H30 are omitted for clarity. Thermal ellipsoids are set at the 30% probability level.

Moreover, $3^+[AlBr_4]^-$ also cyclized with diazomethyl(trimethyl)silane to give product $12^+[AlBr_4]^-$ (^{11}B NMR: 22.6 ppm). Its solid structure confirmed the migration of the trimethylsilyl group from carbon to the nitrogen atom after cycloaddition to form an unprecedented cationic triazaborole skeleton (Fig. 6c).[26] The B1–C30 bond length is 1.462(5) Å and its WBI value is 1.2978, thus confirming the typical double bond character.[27] All five atoms of the BCN_3 ring are perfectly coplanar with the sum of internal pentagon angles of 540°, and the calculated nucleus-independent chemical-shift values of NICS(0) and NICS(1) are −11.0 and −28.2, respectively, supporting its aromatic character.[28] The computational studies reveal that the generation of aromatic 12^+ from isomerization of the non-migrated intermediate is strongly exergonic (−37.1 kcal mol^{-1}) and thus is thermodynamically favorable (Fig. S91†).

Conclusions

Collectively, this work unravels the elementary reactions of a cationic iminoborane, laying the foundation for efficient alternatives to build organoboron species. Employment of aryl and NHC ligands afforded isolable cationic iminoborane 3^+. Both the boron atom and B≡N triple bond in 3^+ could behave as reactive sites for derivatization enabling coordination, addition, and cycloaddition leading to a facile access to three-coordinate boron cations. This clearly confirms that substituent modification could boost the reactivity of cationic iminoboranes since analogous **VII-BPh$_4$** lacks the dipole reactivity toward CO_2,[11] CH_3CN, $H_3N{\cdot}BH_3$ and Me_3SiN_3 (Figs. S76–S78†). These systematic results indicate that unsaturated boron cations, which integrate both Lewis-acidity and multiple bond reactivities, are attractive synthons in organic synthesis. Investigations on the isolation and applications of more functional boron cations are continuously underway in our laboratory.

Data availability

Experimental and computational data has been provided as ESI.†

Author contributions

L. K. designed the study and supervised the project. R. G. synthesized the complexes and conducted most of the measurements. X. Z., L. L. L. and L. K. performed the theoretical calculations. T. L. collected the crystal structures. Q. L. conducted the HRMS measurement. D. A. R., L. L. L., C.-H. T. and L. K. wrote the manuscript. All authors discussed the experimental results and commented on the manuscript.

Conflicts of interest

The authors declare no competing financial interests.

Acknowledgements

We gratefully acknowledge financial support from the National Natural Science Foundation of China (Grants 21971144, 21702228 and 22101114), the Key R&D Program of Shandong Province (Grant 2019GGX102032), the Natural Science Foundation of Shandong Province (Grant ZR2019ZD46), the Qilu Youth Scholar Funding of Shandong University (Grant 11190088963021), the Multidisciplinary Research and Innovation Team of Young Scholars of Shandong University (Grant 2020QNQT007) and the Fundamental Research Funds for the Central Universities (Grant 2021JCG019). The theoretical work is supported by the Center for Computational Science and Engineering as well as CHEM High-Performance Supercomputer Cluster located in the Department of Chemistry at SUSTech. L. L. L. gratefully acknowledges the SUSTech start-up fund (Y01216248). Technical support from the SC-XRD platform of SDU SC&PP research facilities and Prof. Di Sun are acknowledged.

Notes and references

1 For selected reviews, see: (*a*) B. Rao and R. Kinjo, *Chem.–Asian J.*, 2018, **13**, 1279–1292; (*b*) S. Dagorne and R. Wehmschulte, *ChemCatChem*, 2018, **10**, 2509–2520; (*c*) G. I. Nikonov, *ACS Catal.*, 2017, **7**, 7257–7266; (*d*) W. Li, X. Ma, M. G. Walawalkar, Z. Yang and H. W. Roesky, *Coord. Chem. Rev.*, 2017, **350**, 14–29; (*e*) P. Eisenberger and C. M. Crudden, *Dalton Trans.*, 2017, **46**, 4874–4887; (*f*) B. Michelet, S. Tang, G. Thiery, J. Monot, H. Li, R. Guillot, C. Bour and V. Gandon, *Org. Chem. Front.*, 2016, **3**, 1603–1613; (*g*) Y. Sarazin and J.-F. Carpentier, *Chem. Rev.*, 2015, **115**, 3564–3614; (*h*) C. Bour and V. Gandon, *Coord. Chem. Rev.*, 2014, **279**, 43–57; (*i*) T. S. De Vries, A. Prokofjevs and E. Vedejs, *Chem. Rev.*, 2012, **112**, 4246–4282.

2 For selected reviews, see:(*a*) A. Widera, E. Filbeck and H.-J. Himmel, *Eur. J. Inorg. Chem.*, 2020, 3017–3029; (*b*) D. Franz and S. Inoue, *Chem. –Eur. J.*, 2019, **25**, 2898–2926; (*c*) H.-J. Himmel, *Angew. Chem., Int. Ed.*, 2019, **58**, 11600–11617; (*d*) V. Nesterov, D. Reiter, P. Bag, P. Frisch, R. Holzner, A. Porzelt and S. Inoue, *Chem. Rev.*, 2018, **118**, 9678–9842; (*e*) Y.-F. Lin and C.-W. Chiu, *Chem. Lett.*, 2017, **46**, 913–922; (*f*) T. A. Engesser, M. R. Lichtenthaler, M. Schleep and I. Krossing, *Chem. Soc. Rev.*, 2016, **45**, 789–899; (*g*) I. B. Sivaev and V. I. Bregadze, *Coord. Chem. Rev.*, 2014, **270–271**, 75–88; (*h*) S. Dagorne and D. A. Atwood, *Chem. Rev.*, 2008, **108**, 4037–4071; (*i*) W. E. Piers, S. C. Bourke and K. D. Conroy, *Angew. Chem., Int. Ed.*, 2005, **44**, 5016–5036; (*j*) D. A. Atwood, *Coord. Chem. Rev.*, 1998, **176**, 407–430; (*k*) D. Atwood and J. Jegier, *Chem. Commun.*, 1996, 1507–1508; (*l*) P. Kölle and H. Nöth, *Chem. Rev.*, 1985, **85**, 399–418.

3 (*a*) H. Nöth, R. Staudigl and H.-U. Wagner, *Inorg. Chem.*, 1982, **21**, 706–716; (*b*) P. Kölle and H. Nöth, *Chem. Ber.*, 1986, **119**, 313–324.

4 S. Courtenay, J. Y. Mutus, R. W. Schurko and D. W. Stephan, *Angew. Chem., Int. Ed.*, 2002, **41**, 498–501.

5 Y. Shoji, N. Tanaka, K. Mikami, M. Uchiyama and T. Fukushima, *Nat. Chem.*, 2014, **6**, 498–503.

6 (*a*) K. L. Bamford, Z.-W. Qu and D. W. Stephan, *J. Am. Chem. Soc.*, 2019, **141**, 6180–6184; (*b*) C. J. Major, K. L. Bamford, Z.-W. Qu and D. W. Stephan, *Chem. Commun.*, 2019, **55**, 5155–5158; (*c*) K. L. Bamford and D. W. Stephan, *Dalton Trans.*, 2020, **49**, 17571–17577.

7 N. Tanaka, Y. Shoji, D. Hashizume, M. Sugimoto and T. Fukushima, *Angew. Chem., Int. Ed.*, 2017, **56**, 5312–5316.

8 D. Franz, T. Szilvási, A. Pöthig and S. Inoue, *Chem. –Eur. J.*, 2019, **25**, 11036–11041.

9 For ylide or carbodicarbene stabilized boron cations featuring partial B=C double bonds, see:(*a*) W.-C. Chen, C.-Y. Lee, B.-C. Lin, Y.-C. Hsu, J.-S. Shen, C.-P. Hsu, G. P. A. Yap and T.-G. Ong, *J. Am. Chem. Soc.*, 2014, **136**, 914–917; (*b*) T. Scherpf, K.-S. Feichtner and V. H. Gessner, *Angew. Chem., Int. Ed.*, 2017, **56**, 3275–3279.

10 For transition metal substituted boron cations, see:(*a*) H. Braunschweig, K. Radacki and A. Schneider, *Chem. Commun.*, 2010, **46**, 6473–6475; (*b*) H. Braunschweig, K. Kraft, T. Kupfer, K. Radacki and F. Seeler, *Angew. Chem., Int. Ed.*, 2008, **47**, 4931–4933; (*c*) S. Aldridge, C. Jones, T. Gans-Eichler, A. Stasch, D. L. Kays, N. D. Coombs and D. J. Willock, *Angew. Chem., Int. Ed.*, 2006, **45**, 6118–6122; (*d*) H. Braunschweig, K. Radacki and K. Uttinger, *Angew. Chem., Int. Ed.*, 2007, **46**, 3979–3982; (*e*) H. Braunschweig, K. Radacki, D. Rais and D. Scheschkewitz, *Angew. Chem., Int. Ed.*, 2005, **44**, 5651–5654; (*f*) D. L. Coombs, S. Aldridge, C. Jones and D. J. Willock, *J. Am. Chem. Soc.*, 2003, **125**, 6356–6357.

11 F. Dahcheh, D. W. Stephan and G. Bertrand, *Chem. –Eur. J.*, 2015, **21**, 199–204.

12 D. Franz, E. Irran and S. Inoue, *Angew. Chem., Int. Ed.*, 2014, **53**, 14264–14268.

13 For selected reviews, see:(*a*) H. Nöth, *Angew. Chem., Int. Ed. Engl.*, 1988, **27**, 1603–1622; (*b*) P. Paetzold, *Adv. Inorg. Chem.*, 1987, **31**, 123–170.

14 (*a*) R. Guo, J. Jiang, C. Hu, L. L. Liu, P. Cui, M. Zhao, Z. Ke, C.-H. Tung and L. Kong, *Chem. Sci.*, 2020, **11**, 7053–7059; (*b*) P. Cui, R. Guo, L. Kong and C. Cui, *Inorg. Chem.*, 2020, **59**, 5261–5265.

15 (*a*) G. Elter, M. Neuhaus, A. Meller and D. Schmidt-Bäse, *J. Organomet. Chem.*, 1990, **381**, 299–313; (*b*) M. Nutz, B. Borthakur, R. D. Dewhurst, A. Deißenberger, T. Dellermann, M. Schäfer, I. Krummenacher, A. K. Phukan and H. Braunschweig, *Angew. Chem., Int. Ed.*, 2017, **56**, 7975–7979.

16 B. Cordero, V. Gómez, A. E. Platero-Prats, M. Revés, J. Echeverría, E. Cremades, F. Barragán and S. Alvarez, *Dalton Trans.*, 2008, 2832–2838.

17 P. Paetzold, C. von Plotho, G. Schmid, R. Boese, B. Schrader, D. Bougeard, U. Pfeiffer, R. Gleiter and W. Schüfer, *Chem. Ber.*, 1984, **117**, 1089–1102.

18 (*a*) A. R. Jupp, T. C. Johnstone and D. W. Stephan, *Inorg. Chem.*, 2018, **57**, 14764–14771; (*b*) A. R. Jupp, T. C. Johnstone and D. W. Stephan, *Dalton Trans.*, 2018, **47**, 7029–7035.

19 H. Laaziri, L. O. Bromm, F. Lhermitte, R. M. Gschwind and P. Knochel, *J. Am. Chem. Soc.*, 1999, **121**, 6940–6941.
20 A. Ansorge, D. J. Brauer, H. Bürger, T. Hagen and G. Pawelke, *J. Organomet. Chem.*, 1993, **444**, 5–14.
21 (*a*) S. Lau, D. Gasperini and R. L. Webster, *Angew. Chem., Int. Ed.*, 2021, **60**, 14272–14294; (*b*) D. H. A. Boom, A. R. Jupp and J. Chris Slootweg, *Chem. –Eur. J.*, 2019, **25**, 9133–9152.
22 L. Winner, W. C. Ewing, K. Geetharani, T. Dellermann, B. Jouppi, T. Kupfer, M. Schäfer and H. Braunschweig, *Angew. Chem., Int. Ed.*, 2018, **57**, 12275–12279.
23 E. M. Leitao, N. E. Stubbs, A. P. M. Robertson, H. Helten, R. J. Cox, G. C. Lloyd-Jones and I. Manners, *J. Am. Chem. Soc.*, 2012, **134**, 16805–16816.
24 P. Paetzold, E. Schröder, G. Schmid and R. Boese, *Chem. Ber.*, 1985, **118**, 3205–3216.
25 (*a*) M. Nutz, B. Borthakur, R. D. Dewhurst, A. Deißenberger, T. Dellermann, M. Schäfer, I. Krummenacher, A. K. Phukan and H. Braunschweig, *Angew. Chem., Int. Ed.*, 2017, **56**, 7975–7979; (*b*) D. Prieschl, G. Belanger-Chabot, X. Guo, M. Dietz, M. Müller, I. Krummenacher, Z. Lin and H. Braunschweig, *J. Am. Chem. Soc.*, 2020, **142**, 1065–1076.
26 For cationic boroles, see:(*a*) T. Heitkemper and C. P. Sindlinger, *Chem. –Eur. J.*, 2020, **26**, 11684–11689; (*b*) W. Yang, K. E. Krantz, L. A. Freeman, D. A. Dickie, A. Molino, A. Kaur, D. J. D. Wilson and R. J. Gilliard Jr, *Chem. –Eur. J.*, 2019, **25**, 12512–12516; (*c*) C. K. Narula and H. Nöth, *Inorg. Chem.*, 1985, **24**, 2532–2539.
27 A. Berndt, *Angew. Chem., Int. Ed.*, 1993, **32**, 985–1009.
28 B. Su and R. Kinjo, *Synthesis*, 2017, **49**, 2985–3034.